NASA Technical Memorandum 100952
AIAA-88-3025

Hot Gas Ingestion Testing of an Advanced STOVL Concept in the NASA Lewis 9- by 15-Foot Low Speed Wind Tunnel With Flow Visualization

Albert L. Johns
Lewis Research Center
Cleveland, Ohio

and

Joseph D. Flood, Thomas W. Strock, and Kurt C. Amuedo
McDonnell Douglas Corporation
St. Louis, Missouri

Prepared for the
24th Joint Propulsion Conference
cosponsored by the AIAA, ASME, SAE, and ASEE
Boston, Massachusetts, July 11-13, 1988

NASA

HOT GAS INGESTION TESTING OF AN ADVANCED STOVL CONCEPT IN THE NASA LEWIS 9- BY 15-FOOT LOW SPEED WIND TUNNEL WITH FLOW VISUALIZATION

Albert L. Johns
National Aeronautics and Space Administration
Lewis Research Center
Cleveland, Ohio 44135

and

Joseph D. Flood, Thomas W. Strock, and Kurt C. Amuedo
McDonnell Aircraft Company
McDonnell Douglas Corporation
St. Louis, Missouri 63166

SUMMARY

Advanced Short Takeoff/Vertical Landing (STOVL) aircraft capable of operating from remote sites, damaged runways, and small air capable ships are being pursued for deployment around the turn of the century. To achieve this goal, it is important that the technologies critical to this unique class of aircraft be developed. Recognizing this need, NASA Lewis Research Center, McDonnell Douglas Aircraft, and DARPA defined a cooperative program for testing in the NASA Lewis 9- by 15-Foot Low Speed Wind Tunnel (LSWT) to establish a database for hot gas ingestion, one of the technologies critical to STOVL.

This paper will present results from a test program along with a discussion of the facility modifications allowing this type of testing at model scale. These modifications to the tunnel include a novel ground plane, an elaborate model support which included 4° of freedom, heated high pressure air for nozzle flow, a suction system exhaust for inlet flow, and tunnel sidewall modifications. Several flow visualization techniques were employed including water mist in the nozzle flows and tufts on the ground plane. Headwind (freestream) velocity was varied from 8 to 23 kn.

E-4250

INTRODUCTION

Supersonic Advanced Short Takeoff/Vertical Landing aircraft capable of operating from remote sites, damaged runways, and ships (fig. 1) are being pursued for deployment around the turn of the century. To achieve this goal, it is important that the technologies critical to this unique class of aircraft be developed. Several of the Advanced Short Takeoff/Vertical Landing concepts have the problem of hot gas ingestion (during vertical flight operation while in ground effect) as a key development issue.

In general, Short Takeoff/Vertical Landing aircraft operation near the ground can be subject to significant thrust losses due to the ingestion of hot exhaust gases and induced jet/airframe iterations (refs. 1 and 2). These interactions occur between the lift jets, entrained flow over the aircraft surfaces and along the ground, and ambient winds (fig. 2). In the development of efficient Short Takeoff/Vertical Landing aircraft, it is essential to minimize

losses caused by ground effects to prevent compromising the performance and overall mission of the aircraft. Therefore, those factors which substantially affect hot gas ingestion and induced lift must be identified and a comprehensive database must be established to guide the design of advanced short takeoff/vertical landing aircraft. Performing this type of research at full scale, where it has classically been done, is difficult and expensive. A wind tunnel capability is therefore both desired and required. Hot gas testing at model scale has been attempted previously in a wind tunnel (ref. 1) but sometimes with less than satisfactory results. Tunnel wall interference, premature model and tunnel heating, and temperature scaling problems all have influenced the results. Knowing these past shortcomings NASA Lewis Research Center, McDonnell Douglas Aircraft, and DARPA defined a cooperative program for testing in the NASA Lewis 9- by 15-Foot Low Speed Wind Tunnel (LSWT) to develop a new model testing technique and establish a required database for hot gas ingestion for advanced STOVL. This paper will present results from this test program along with a discussion of the facility modifications allowing a successful completion of this type testing at model scale. These modifications to the tunnel include a novel ground plane, an elaborate model support which included 4° of freedom, heated high pressure air for nozzle flow, a suction system for inlet flow, and tunnel sidewall modifications. Several flow visualization techniques were employed including water mist in the nozzle flows and tufts on the ground plane.

FACILITY

The tests were conducted in the NASA Lewis 9- by 15-Foot LSWT which is located in the return leg of the 8- by 6-Foot Supersonic Wind Tunnel (fig. 3). Some tests were conducted at headwind velocities from 30 to 90 kn. These velocities were obtained using the compressor and by sliding doors 1 and 2 from full open to full closed. The majority of the tests were conducted from 8 to 23 kn. These lower velocities were obtained using the blowers located in the dryer building and by changing the opening of doors 4 and 5. During the foregoing operation, doors 1 and 2 remain closed.

MODEL AND CONFIGURATIONS

The model shown in figure 4 is a 9.2 percent scale model of the MCAIR 279-3C concept. The model is basically made up of three main sections; the forward, center, and aft fuselage.

Forward Fuselage

The forward fuselage section consists of the nose cone, the inlets (both main and auxiliary), nose gear, canards, canopy, and compressor face rake assembly. Details of the compressor rake are shown in figure 4(b). The compressor face rake instrumentation locations are shown in table I.

Center Fuselage

The center fuselage section consists of both forward and aft nozzles and the related plenums, the inlet suction duct, the main landing gear, and the lift improvement devices (LIDs) (when so installed) (fig. 5).

The LIDs consist of a forward fence, sidewalls, and longitudinal strakes located around the nozzles perimeter (fig. 5).

Aft Fuselage

The aft fuselage consists of a cover and lower body.

Configuration

Figure 6(a) shows the front view of the forward nozzles. In this plane, the nozzles can be rotated inboard to form a negative splay angle (from the straight down position, 0° splay). The aft nozzles were always at 0° splay. From the side view (fig. 6(b)), the nozzles (forward and aft) can be rotated from 0° (full aft) to 100° (nozzles are pointed slightly forward). The angle created in the side view is referred to as vector angle.

MODEL-SUPPORT SYSTEMS - INSTRUMENTATION

A view of the model in the test section is shown in figure 7. Also shown are the model support system, which includes the high pressure hot (500° F) air lines; a suction line to provide inlet airflow, and the ground plane with the sliding trap door open. The model height was varied by changing the number of spacers between the upper and lower flanges and adjusting the jack screws.

The high pressure air lines provided the air flow for the model nozzles. The suction duct also provided support for the hot air and instrumentation lines. Pitch, roll, and yaw were adjusted by changing the position of the ball joint, located below the lower flange.

Ground Plane

As seen in the photograph of figure 7 and shown in the schematic of figure 8, an elevated ground plane was installed in the test section which incorporated a unique trap door feature. The ground plane was installed 18 in. above the test section floor. This kept the hot airflow off the tunnel floor and allowed instrumentation for pressure and temperature measurement on the ground plane.

Tufts were placed on the ground plane (fig. 7), for flow visualization. Ground plane instrumentation locations are given in table II.

Trap Door Scavenging System

A trap door scavenging system was installed to prevent the model surfaces and ground plane from artificially heating while the nozzles temperature and pressure conditions were being set between data points. The unique trap door system consists of three main components: sliding trap door (fig. 8), ducting, and ejectors (fig. 9). Model nozzle flow was sucked through the trap door opening, down the duct under the ground plane; and exhausted downstream of the test section by the ejectors (fig. 9). When a data point was taken, the trap door was closed and the ejectors were automatically shut off. After taking the data point, the trap door was opened and the ejectors were automatically turned on. The trap door was pneumatically actuated, and it closed in approximately 0.5 sec.

Sidewall Bleed System

A sidewall bleed system prevented the hot air flow of the nozzles from recirculating in the test section. Two rows of acoustic panels were removed from each sidewall at the ground plane height along the length of the test section (fig. 10). This allowed the ground airflow moving to the sidewalls to flow out of the test section into the surrounding cavity as shown in figure 10.

Water Injection System

A water injection system was used to conduct flow visualization testing. Water was injected into unheated nozzle flow where it was atomized. Porous plates located in the nozzle air supply lines helped to atomize the flow. White light illumination was used to allow the flow field to be visualized. A simplified schematic of the water injection system is shown in figure 11.

Instrumentation

A propeller anemometer was used to measure air flow velocity in the test section as shown in figure 12. The propeller anemometer is capable of measuring headwind velocities from 1 to 98 kn. The propeller measuring accuracy was ±0.6 kn.

The tunnel reference temperature, against which all temperature rises were computed, was measured immediately upstream of the test section (in the vicinity of door 3 (fig. 3)). Two iron/constantan (I/C) thermocouples, one on each wall of the tunnel, were used to measure the freestream temperature and were averaged to compute the reference temperature.

Seven 20 ft strips of 10 thermocouples were mounted within the test section (fig. 13). One strip had I/C's and the others were chrome/alumel (C/A) thermocouples. These strips measured the heating in the test section. Two strips were placed on each sidewall and three strips in the ceiling. The ceiling also contained a 8.5 ft strip of static pressure instrumentations for obtaining static measurements. Details of the thermocouples and pressure strips are shown in figure 14.

The ground plane and trap door thermocouples measured air temperature. Pressure taps were located on both the ground plane and trap door. The ground plane coordinate system in reference to the model is shown in figure 15.

The NASA Lewis ESCORT III data system was used for data acquisition. This system has a scan update rate every second which includes all data reduction computations and facility and model measurements. The electronically scanned pressure system (ESP) consists of fourteen modules, each of which contained 32 individual transducers. Three ranges of transducers were used: (1) ±5 psid with an accuracy of ±0.007 psi, (2) ±15 psid with an accuracy of ±0.02 psi, (3) +250 psid with an accuracy of ±0.17 psi.

TEST PROCEDURE

All test runs were conducted at steady state conditions with the model configuration and attitude fixed. The model configuration and attitude (pitch, yaw, roll, and height) were set manually. As stated earlier, most of the test was conducted from 8 to 23 kn. This is the headwind velocity range for vertical landing. In general, the following depicts a typical test run:

(1) A pretest tare reading was taken to verify instrumentation operation.

(2) The trap door-ejector system was activated (trap door open and ejectors running).

(3) The inlet suction flow was set to the maximum compressor face Mach number.

(4) The nozzle air supply system was activated and each nozzle was set to a nozzle pressure ratio of approximately 4.0 to heat the model.

(5) The natural gas heater was brought up to maximum temperature at the nozzles plenum (960° R).

(6) After reaching the desired nozzle temperature, the inlet suction flow, nozzle pressure ratios and temperature were set to a test condition. The desired headwind velocity was set and a reference data point was taken with the trap door open.

(7) The trap door was then closed and the inlet temperature rise versus time was monitored on a scrolling video plot to establish steady state condition. At steady state condition data are taken. It can take 15 to 45 sec to reach steady state conditions at the compressor face rake.

(8) After the completion of the data recording, the trap door is opened and the next condition is set.

(9) At the conclusion of a test run a post tare reading is taken.

PRESENTATION OF EXPERIMENTAL RESULTS

The primary objectives of this paper are to convey the modifications to the 9- by 15-Foot Low Speed Wind Tunnel and some of the results obtained for the STOVL hot gas ingestion test. In order to show these results, it is necessary to start the discussion with the tunnel modifications, followed by the model HGI results. A discussion on the ground plane temperature and pressure distributions will follow. The final figures will show a few frames from the water flow visualization.

Several parameters are important in hot gas ingestion. For example, the inlet temperature distortion can cause engine stall; and the inlet pressure recovery is indicative of the engine thrust. However, this report will use the inlet temperature rise, which is the increase in the compressor face temperature over a reference temperature. The effect of the inlet temperature rise is a reduction in the engine thrust. Inlet temperature can be influenced by several factors such as headwind, height above the ground, splay angle between the forward nozzles, nozzle temperature levels, and nozzle pressure ratio.

This report will address the effect of splay angle, lift improvement devices (LIDs), and main landing gear height above the ground plane.

RESULTS AND DISCUSSION

As was discussed previously in figure 2, hot gas ingestion (HGI) is caused by two sources. The first is the near field ingestion which is a result of the fountain upwash. With multinozzles, the nozzle jets impinge on the ground spreading in all directions. The inward flowing ground flow (from a nozzle) encounters other inward flowing ground flow from another nozzle. These flows meet forming a fan shape upwash or "fountain." Once it encounters another jet, both flow upward forming a fountain. At some given model height above the ground, the fountain flow will impinge on the undersurface of the model. At this point, the near field hot gas ingestion occurred. This hot gas can flow forward and get ingested into the inlet.

The air flowing along the axis has not mixed and generally results in a high inlet temperature rise. The fountain upwash strength is determined, in part, by the forward nozzles thrust splay angle, the nozzles exit plane spacing, and the height of the model above the ground plane. A variation of any one of these can change the strength of the fountain. The exit plane spacing establishes the relative flow area available for the central fountain to flow forward along the underside of the model. This will determine the amount of hot gas that is ingested into the inlet flow field and get pulled into the inlet.

The other source of hot gas ingestion is the far field. The high velocity ground jet from the nozzles flow ahead of the model until, due to buoyancy and the headwind, the flows separate from the ground. The flow is then blown back to the model inlet flow field where the hot gas is ingested into the inlet. This form of HGI generally causes a lower inlet temperature rise in comparison to the near field HGI. The exception is when the far field separation occurs at the inlet.

The clean configuration was tested to provide a baseline configuration to compare the effect of LIDs. The clean configuration will generally have a higher inlet temperature rise because it has no way of diverting the near field ingestion. A parameter of critical value for vertical landing concept is the height the main landing gear is above the ground plane. Data presented in this paper are for the design condition of a nozzle pressure ratio of 3.02 and compressor face Mach number of 0.40. The nozzle pressure ratio was varied from 1.1 to 4.00.

The inlet temperature rise at the compressor face versus the distance of the main landing gear wheel above the ground plane is shown in figure 16.

The results are shown for the clean configuration; -6° splay on the forward nozzles and 0° splay on the aft nozzles. The data shown for nozzle pressure ratio of 3.02, compressor face Mach number of 0.40, a nozzle exhaust temperature of 960 °R, and a headwind velocity of 10 kn. Inlet temperature rise increases with decreasing height above the ground plane. The most significant point is the ground effect range being relatively small. In general, an increase in headwind velocity will result in a higher level of hot gas ingestion. This is caused by the far field separation occurring closer to the inlet.

The effect of splay angle is shown in figure 17. These results show the inlet temperature rise over a range of headwind velocities. Two clean configurations are shown, one with 0° splay and another with -6° splay (forward nozzles). Again, the data are shown for the design condition and a nozzle exhaust temperature of 960° R. The 0° splay configuration inlet temperature rise was higher than the -6° splay configuration. The difference ranging from 22° at 10 kn to 12° at 23 kn. The 0° splay configuration maximum compressor face temperature rise occurred at the 8 kn headwind condition. It was observed from the flow visualization that the far field separation point occurred near the nose gear. As the headwind velocity increased the separation zones (far and near field) moved under the model, hence producing a reduction in the compressor face temperature rise.

When the LIDs are installed on the -6° splay configuration (fig. 18), the inlet temperature rise is significantly reduced. This reduction was caused by the LIDs effectiveness at containing the fountain upwash and deflecting the hot gas away from the inlet flow field. The LIDs reduced the inlet temperature rise by approximately 52° over the headwind velocity range from 10 to 23 kn.

MODEL TEMPERATURE PROFILES

The air around the model fuselage was measured with thermocouples which protrude 0.10 in. beyond the model surface. Data are shown for the -6° splay configuration with and without LIDs. Air temperature was measured at 43 different locations around the model.

Temperature measurements made 0.10 in. beyond the undersurface of the model are shown in figure 19. These measurements are made along the model centerline. The data are presented for a 10 kn headwind, a nozzle pressure ratio of 3.02, compressor face Mach number of 0.40, and main gear height of 0.10 in. Both configurations had maximum temperature near the main landing

gear of 900 °R. The temperature level was the same for both configurations until upstream of the LIDs forward fence (model station 24). The local temperature was reduced by 200 °R at the forward fence. In the region of the inlet (model stations 10 to 15), the LIDs reduced the temperature by approximately 100 to 150 °R. Therefore, the LIDs were effective in containing and deflecting the hot air flow which impinged on the underside of the model, thereby reducing the degree of HGI.

Temperature measurements made around the perimeter of the main inlet section are shown in figure 20. The results are shown with and without LIDs configurations at the design condition. The LIDs configuration is 100 to 150 °R lower than the clean configuration.

GROUND PLANE AIR TEMPERATURE AND PRESSURE MEASUREMENTS

As noted in the instrumentation section, the ground plane thermocouples measured air temperature. The ground plane temperature distribution along the centerline is presented in figure 21 for the design condition, a nozzle exhaust temperature of 960 °R, a main landing gear height of 0.10 in., and a headwind velocity of 10 kn. Figure 21 shows a comparison of the configurations with and without LIDs. The purpose of the LIDs is to redirect the fountain flow back onto the ground plane region. As a result, the ground flow is slightly intensified between 10 and 50 in. upstream of the mid nozzles location. The ground plane air temperature upstream of the LIDs increases as shown in figure 21. This data tends to indicate that the LIDs can also modify the far field ingestion.

A typical pressure change distribution along the centerline of the ground plane is presented in figure 22 for a 10 kn headwind, and design condition. The nozzle exhaust flow impinges on the ground plane between -10 and +10 in., resulting in a local stagnation pressure near the nozzle total pressure at impingement. The negative pressure change region located under the model is a result of the ground flow acceleration away from the impingement zone and overexpanding. These negative pressures affect the model undersurface, resulting in negative suckdown forces which are seen in the jet induced lift (ref. 1). However, the fountain impinging on the undersurface of the model would result in an upwash force. In general, the four poster configuration tested has a net upwash force (using empirically predicted jet-induced lift characteristics) when in ground effects at a nozzle pressure ratio of 3.02.

A typical far field separation is shown using water flow visualization in figure 23. The tufts on the ground plane pointing toward the model are upstream of the ground jet separation zone, under the influence of the headwind velocity. The tufts pointing away from the model are downstream of the ground jet flow separation zone, under the influence of the nozzles flow. The influence of the ground jet is confined laterally by the freestream (headwind) velocity, due to the lateral velocity decay. This can be observed at the top of figure 23. The tufts in the upper region are pointing downstream (in the direction of the model). The water mist flow visualization have been effective in highlighting the far field ingestion zones/regions of ground plane separation.

Characteristics typical of the near field hot gas ingestion are shown in figure 24. This is a three-quarter view of the clean configuration with a -6° splay. When the ground air flow from two jets meet, a fountain is formed. If there are more than two jets, a fountain is formed between each pair and a central fountain is formed when the flow from all four nozzles meet.

Between the forward and aft nozzles is a stagnation line. The central fountain can also be seen in the aft region under the model. The water mist flow visualization is very effective in showing the near field hot gas ingestion characteristics. The experimental and flow visualization results indicate that the modifications made to the 9- by 15-Foot LSWT effectively validated this facility as an acceptable wind tunnel, for STOVL hot gas ingestion testing.

SUMMARY OF RESULTS

An experimental investigation was conducted in the NASA Lewis 9- by 15-Foot Low Speed Wind Tunnel to determine the effects of Hot Gas Ingestion on a vectored thrust STOVL concept, to build a hot gas ingestion database, and to establish the wind tunnel as an acceptable hot gas testing facility.

The test was conducted with a 9.2 percent scale model. Data were obtained for nozzle pressure ratio ranging from 1.1 to 4.0, inlet Mach number ranging from 0.1 to 0.40, and main landing gear height above the ground plane ranging from -0.20 (wheels removed) to 15.47 in. The model attitude range was as follows: pitch angle +6.5°; yaw angle 0°, 45°, and 90°; and roll angle 0°. Headwind (freestream) velocity was varied form 8 to 23 kn. Several modifications were made to the 9- by 15-Foot LSWT in an effort to validate this hot gas testing facility. The following results were obtained:

(1) The modifications made to the 9- by 15-Foot Low Speed Wind Tunnel have proven to be effective in testing vectored thrust concepts.

(2) The 9- by 15-Foot LSWT has been validated as an acceptable wind tunnel for STOVL hot gas ingestion testing.

(3) LIDs significantly reduced the inlet temperature rise at the compressor face.

(4) Inlet temperature rise increases with decreasing height above the ground plane.

(5) Splay angle can reduce the inlet temperature rise at the compressor face.

(6) The water mist flow visualization results have been very effective in showing both the near and far field ingestion zones, regions/locations of ground plane separation, and jet fountains.

CONCLUDING REMARKS

As a result of the successful program, a large data base has been established for supersonic and subsonic jets exhausting into a subsonic flow field.

A follow-on activity is, therefore recommended and should incorporate further improvements in the 9- by 15-Foot LSWT for HGI-type testing. For example:

(1) A model Integrated Support System (MISS) will be installed. This support system will have 4° of freedom (pitch, roll, yaw, and vertical variation) remotely actuated from the control room. The MISS will have the following features: pitch angle ±20°, angle-of-yaw ±180°, and angle-of-roll ±10°. The height variation will range from wheels-on-ground to approximately 4.5 ft above the present ground plane. The MISS will simulate both inlet and nozzle airflows.

(2) Installation of a thermovision system with both video and digital output.

(3) Installation of a laser sheet system coupled with a standard and U-matic video systems.

(4) A new 1660 °R heated air supply system will be used.

(5) On-line acoustic analysis system will be used.

(6) A new analog system will approximately double the present analog measurement capabilities of the 9- by 15-Foot Low Speed Wind Tunnel.

REFERENCES

1. "Proceedings of the 1985 Ground-Effects Workshop," NASA Ames Research Center, Aug. 20-21, 1985, NASA CP-2462.

2. Strock, T., Amuedo, K., and Flood, J., "Hot Gas Ingestion Test Results of a Four-Poster Vectored Thrust STOVL Concept," NASA CR-182115, July 1988.

TABLE I. - GROUND PLANE INSTRUMENTATION LOCATIONS

[Dimensions are in inches; x measured from trap door leading edge; y is located 22 in. above the ground plane centerline.

z1 panel						y1 panel					
Static pressure			Surface air temperature			Static pressure			Surface air temperature		
x	y	y^{-4}	x	y	y^{-4}	x	y	y^{-4}	x	y	y^{-4}
37.33	22.00	18.00	31.36	22.00	18.00	113.32	22.00	18.00	109.68	-----	18.00
28.37	↓	↓	25.33	↓	↓	107.32	↓	↓	97.74	-----	↓
22.40			19.38			101.32			85.71	-----	
16.40			13.38			95.29			73.74	-----	
10.38			7.34			83.31			------	-----	-----
4.36			3.30			71.31			------	-----	-----
						59.28			------	-----	-----
						47.37			------	-----	-----

TABLE II. - COMPRESSOR FACE RAKE INSTRUMENTATION LOCATIONS

Leg identification			Leg identification		
Number	Angle, deg	Radius, R, in.	Number	Angle, deg	Radius, R, in.
1	66.499		2	21.533	
4	293.501		3	338.467	
5	246.499		6	201.533	
8	113.501		7	158.467	
		0.624			0.624
		.698			.646
		1.081			1.081
		1.209			1.119
		1.396			1.396
		1.56			1.444
		1.651			1.651
		1.81			1.709
		1.872			1.938
		Surface[a]			Surface[a]

[a]Surface denotes static pressure location.

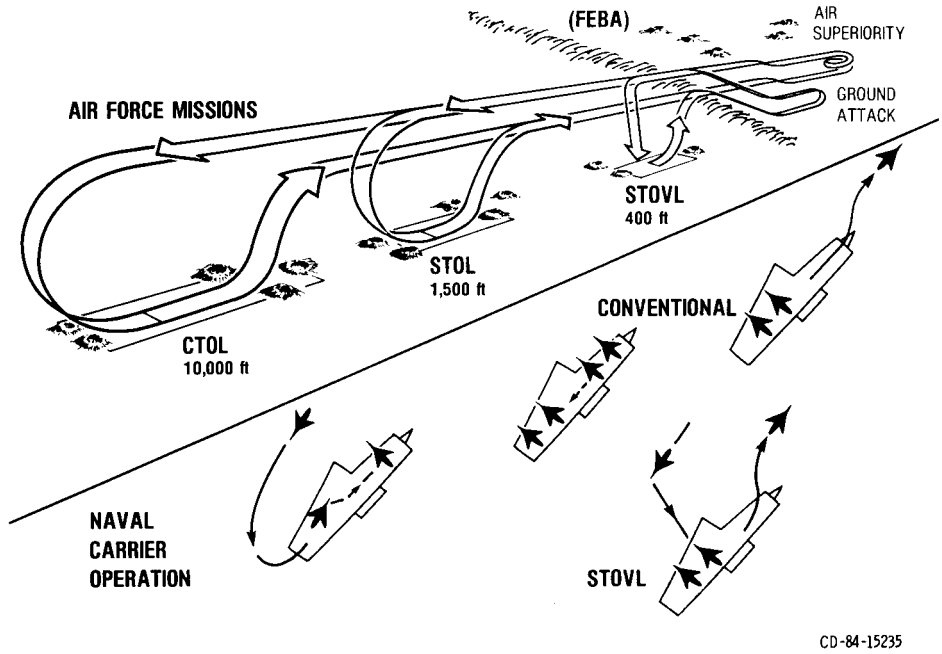

FIGURE 1. - STOVL IMPROVES OPERATIONAL EFFECTIVENESS.

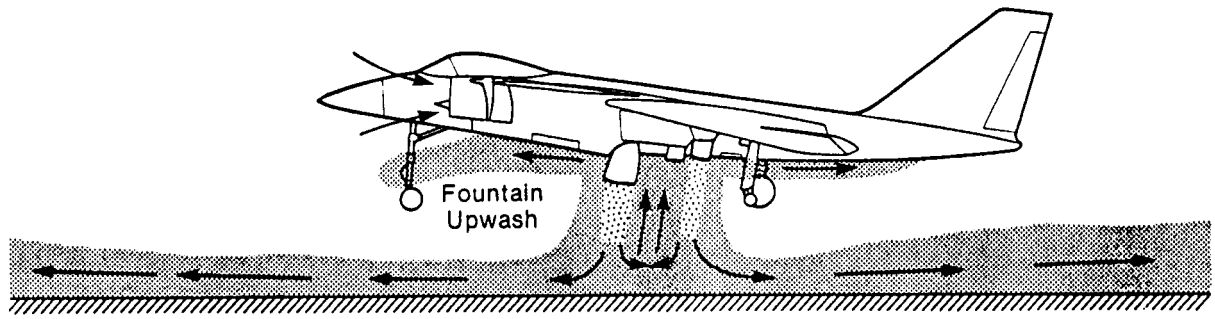

Near Field Hot Gas Ingestion Due to Fountain Upwash

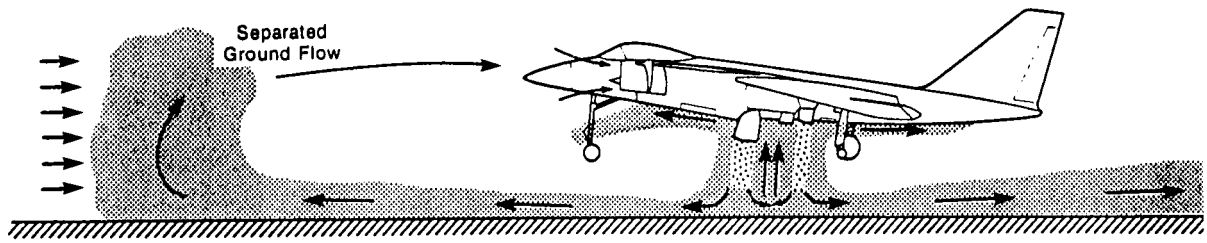

Far Field Hot Gas Ingestion Due to Separated Ground Flow

FIGURE 2. - THE SOURCES OF HOT GAS INGESTION.

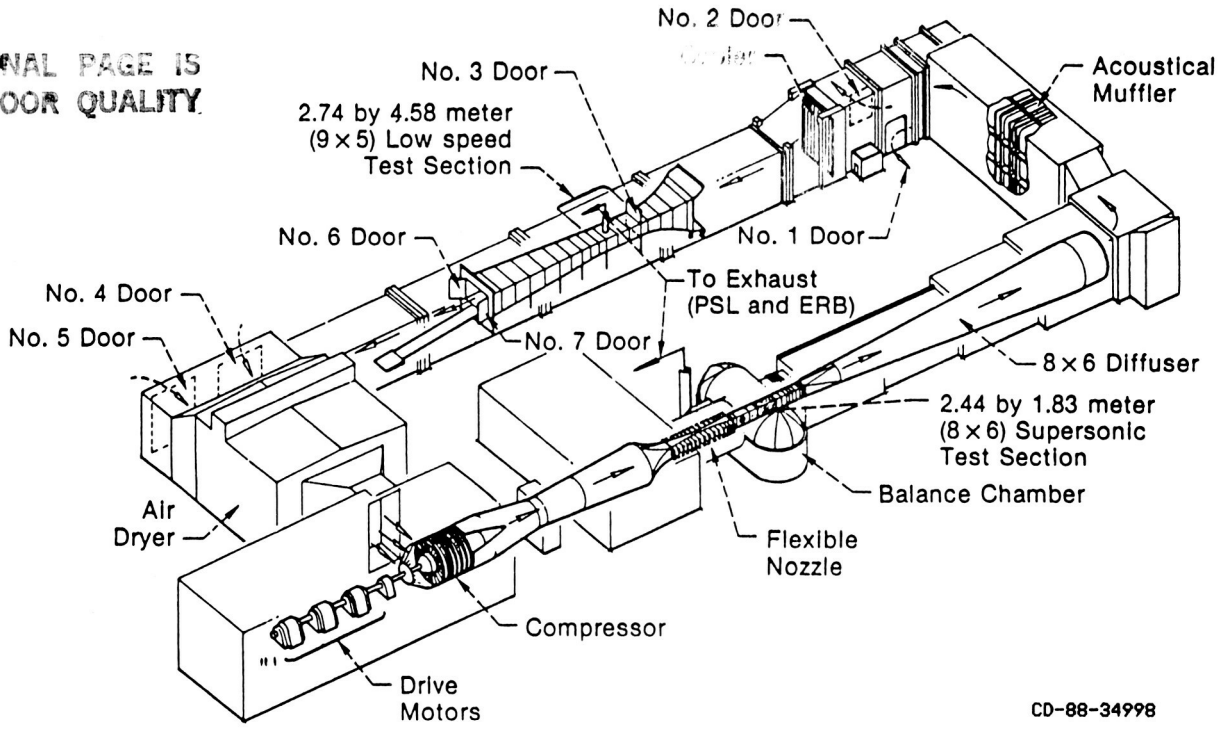

FIGURE 3. - AN ILLUSTRATION OF THE 9- BY 15-FOOT LOW-SPEED WIND TUNNEL AND THE 8- BY 6-FOOT SUPERSONIC WIND TUNNEL.

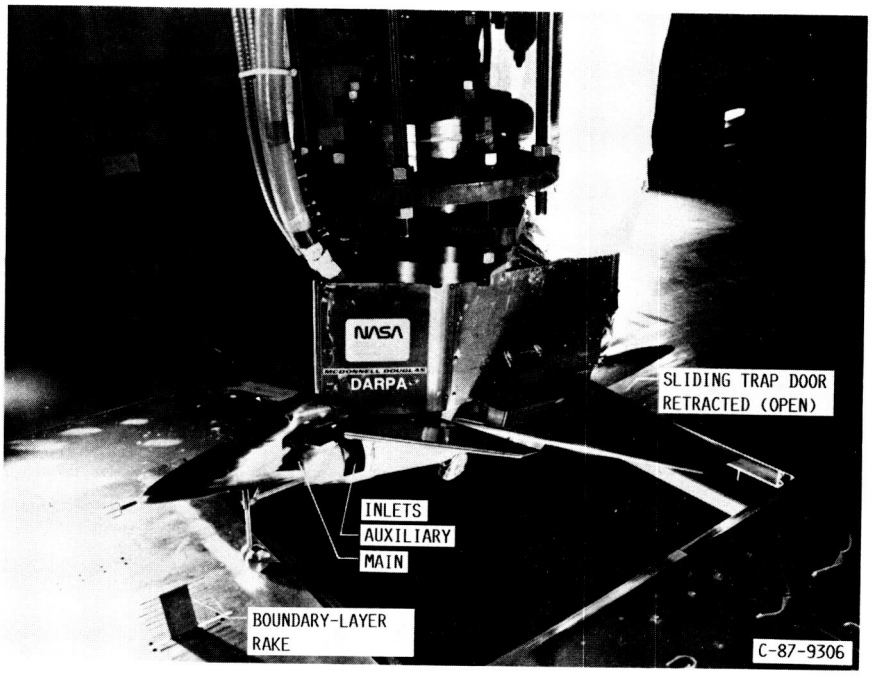

(a) A THREE-QUARTER VIEW OF THE MODEL INSTALLED IN THE 9- BY 15-FOOT LOW-SPEED WIND TUNNEL.

FIGURE 4. - MODEL 279-3C AND COMPRESSOR FACE RAKE DETAILS.

TABLE I. - COMPRESSOR FACE RAKE INSTRUMENTATION LOCATIONS.

Leg Identification			Leg Identification		
Number	Angle, deg.	Radius, R, in.	Number	Angle, deg.	Radius, R, in.
1	66.499		2	21.533	
4	293.501		3	338.467	
5	246.499		6	201.533	
8	113.501		7	158.467	
Total	Temperature	0.624	Total	Temperature	0.646
	Pressure	0.698		Pressure	0.722
	Temperature	1.081		Temperature	1.119
	Pressure	1.209		Pressure	1.251
	Temperature	1.396		Temperature	1.444
	Pressure	1.56		Pressure	1.615
	Temperature	1.651		Temperature	1.709
	Pressure	1.81		Pressure	1.875
	Temperature	1.872		Temperature	1.938
Static	Pressure	2.038	Static	Pressure	2.038

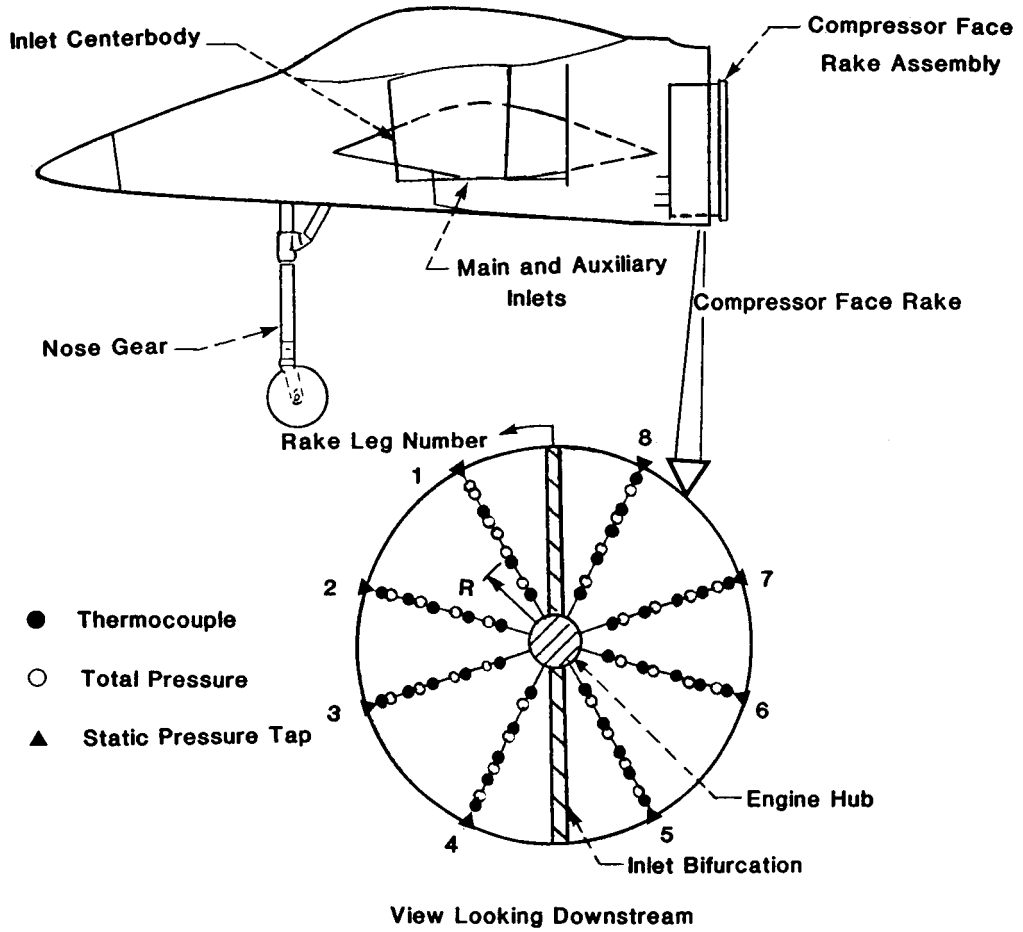

(b) FORWARD FUSELAGE - COMPRESSOR FACE RAKE SCHEMATIC.

FIGURE 4. - CONCLUDED.

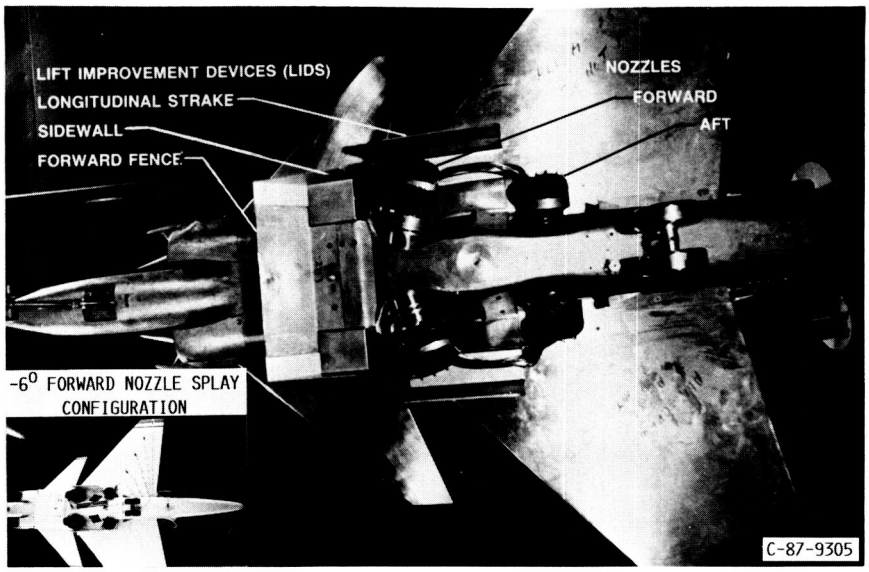

FIGURE 5. - THE UNDERSURFACE OF THE HGI MODEL SHOWING LIDS AND NOZZLES.

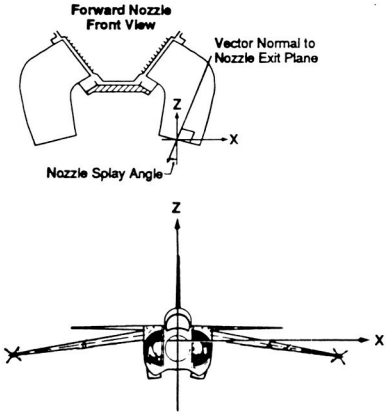

(a) NOZZLE SPLAY ANGLE.

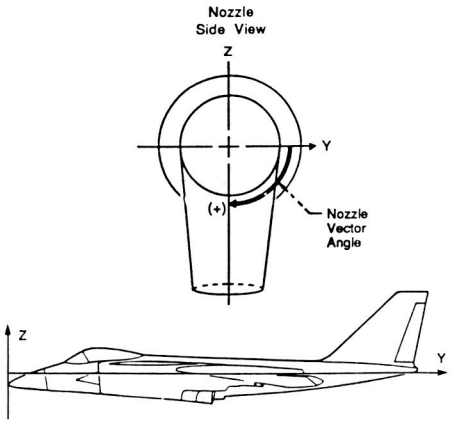

(b) NOZZLE VECTOR ANGLE.

FIGURE 6. - DEFINITION OF FORWARD NOZZLES SPLAY AND VECTOR ANGLES.

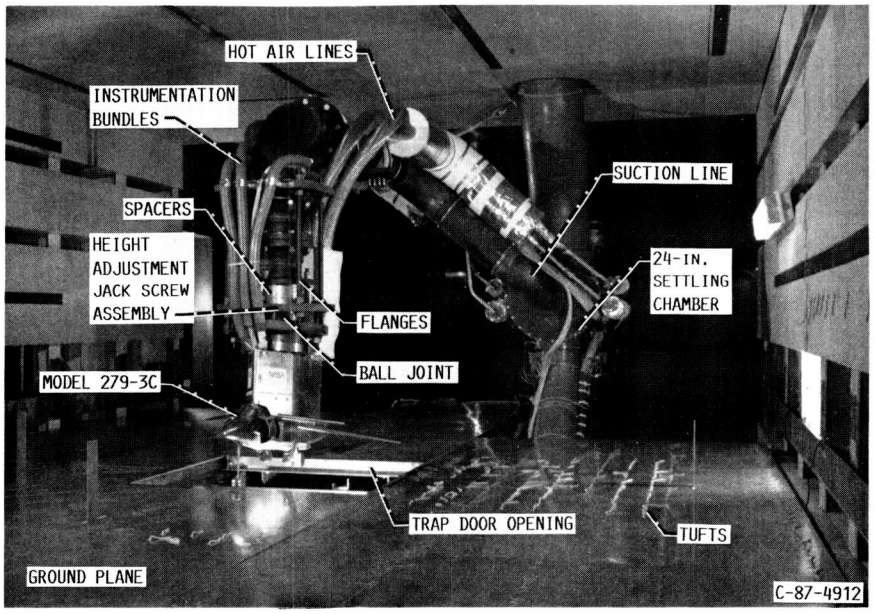

FIGURE 7. - THE HOT GAS INGESTION MODEL AND SUPPORTING SYSTEM INSTALLED IN THE 9- BY 15-FOOT LOW-SPEED WIND TUNNEL.

Table II. - Ground plane instrumentation locations.

Z1 panel — Centerline row

	Static pressure x	Static pressure y
1	37.33	22
2	28.37	21.98
3	22.4	21.94
4	16.4	21.97
5	10.38	21.98
6	4.36	22

	Temperature x	Temperature y
1	31.38	21.97
2	25.34	21.98
3	19.37	21.98
4	13.41	22
5	7.37	21.97
6	3.32	

4" above centerline

	Static pressure x	Static pressure y
1	37.31	18
2	28.34	18
3	22.36	17.97
4	16.36	18.04
5	10.37	18.02
6	4.34	18.04

	Temperature x	Temperature y
1	31.36	17.99
2	25.33	18
3	19.38	17.99
4	13.38	18
5	7.34	18
6	3.3	

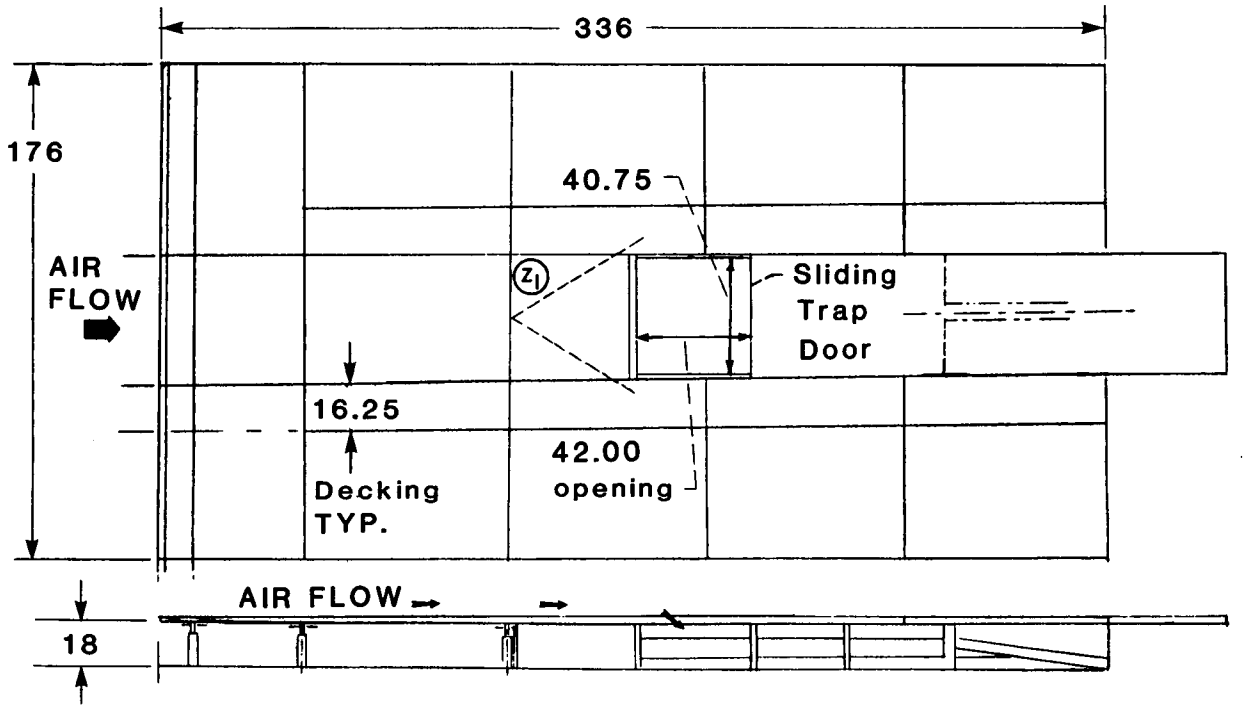

FIGURE 8. - GROUND PLANE SCHEMATIC AND INSTRUMENTATION. (DIMENSIONS IN INCHES.)

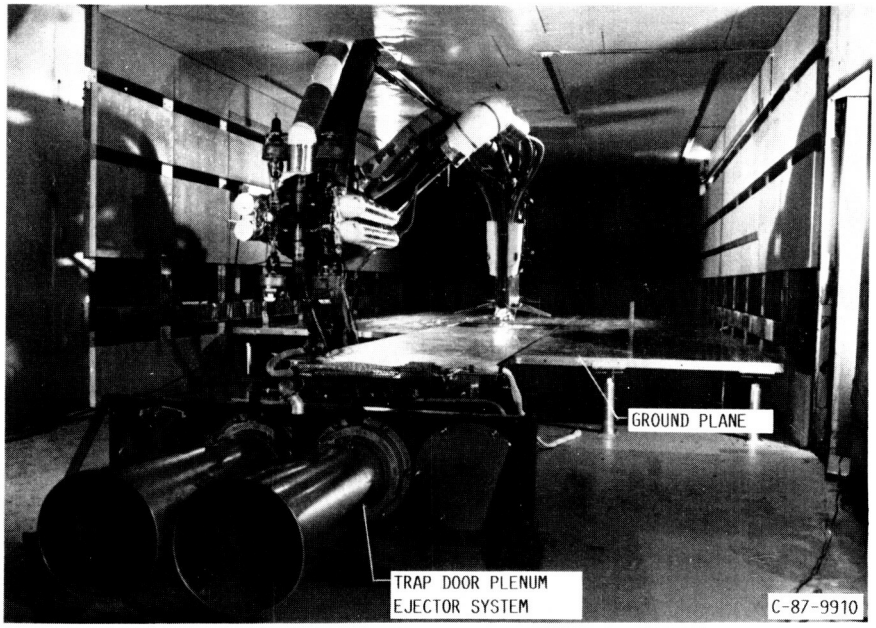

FIGURE 9. - AFT VIEW OF THE 9- BY 15-FOOT LOW-SPEED WIND TUNNEL TEST SECTION.

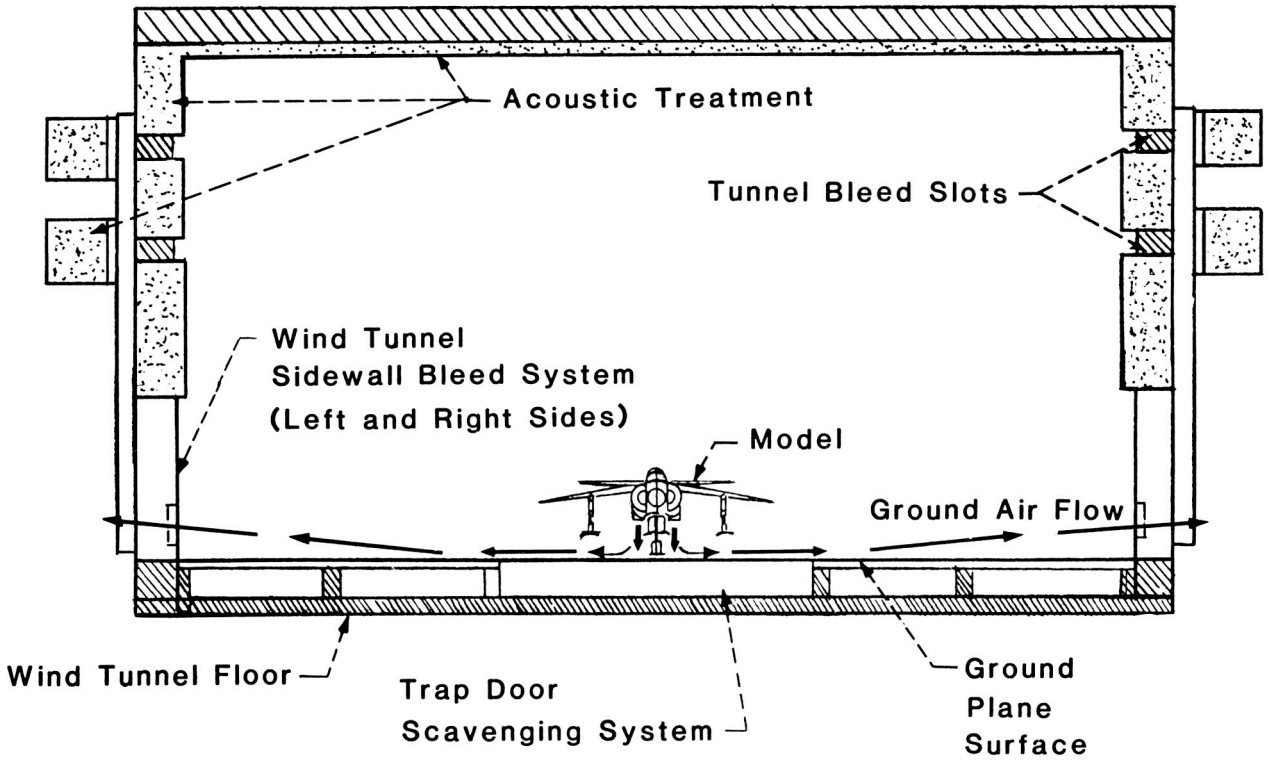

FIGURE 10. - CROSS SECTION OF TEST SECTION SHOWING THE SIDEWALLS SCAVENGING SYSTEM.

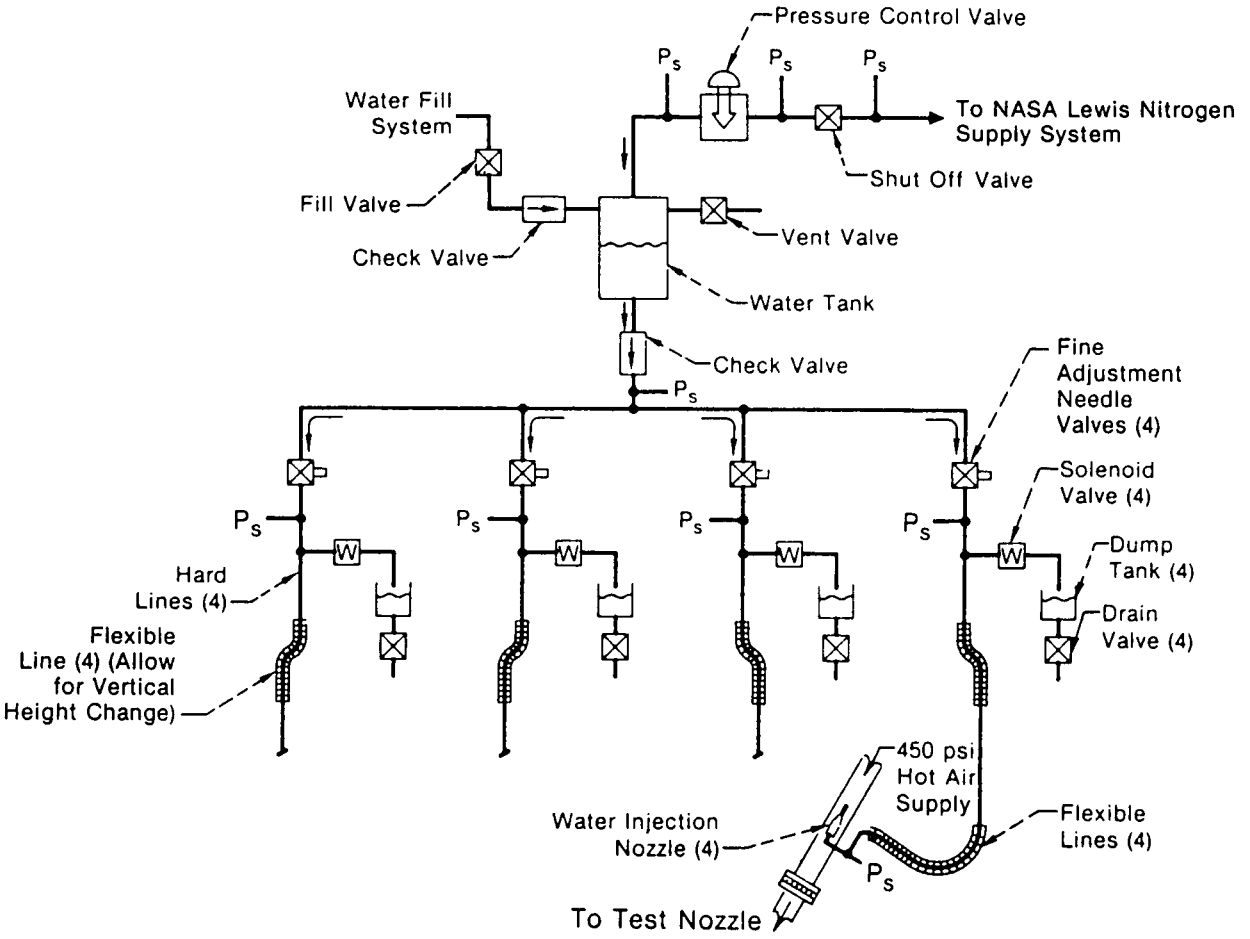

FIGURE 11. - A SCHEMATIC OF THE MODEL FLOW VISUALIZATION WATER INJECTION SYSTEM.

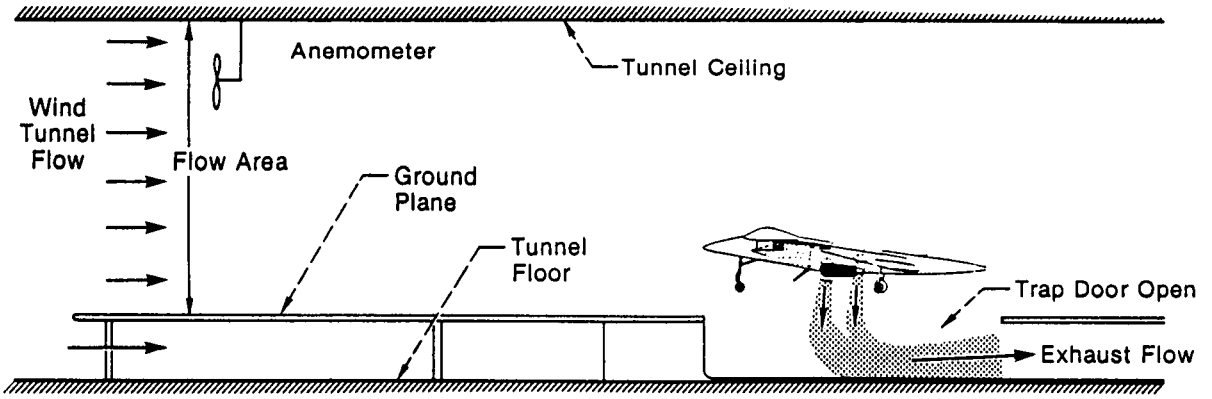

FIGURE 12. - TEST SECTION AIRFLOW VELOCITY MEASURING SYSTEM.

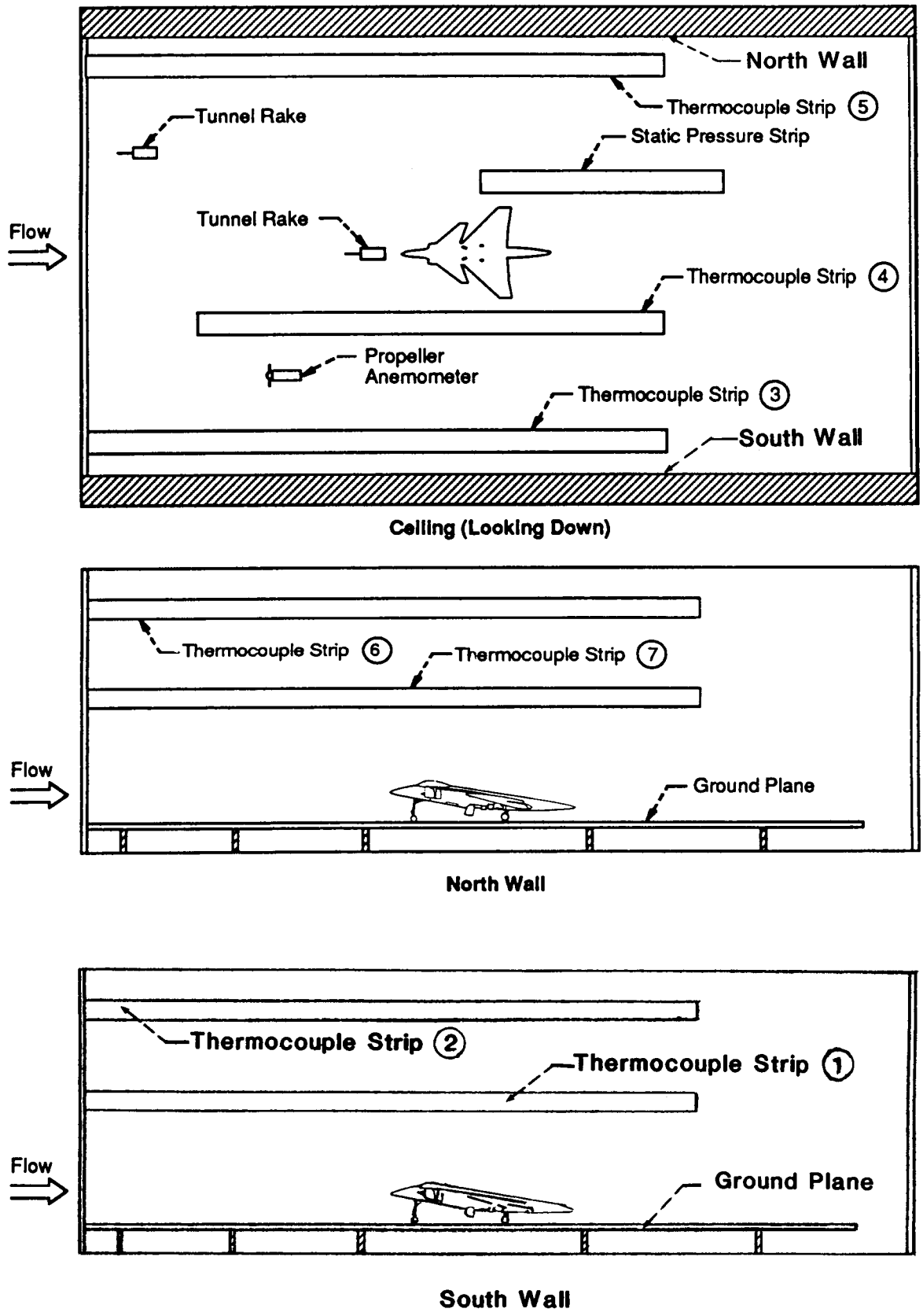

FIGURE 13. - TEST SECTION WALLS AND CEILING INSTRUMENTATIONS.

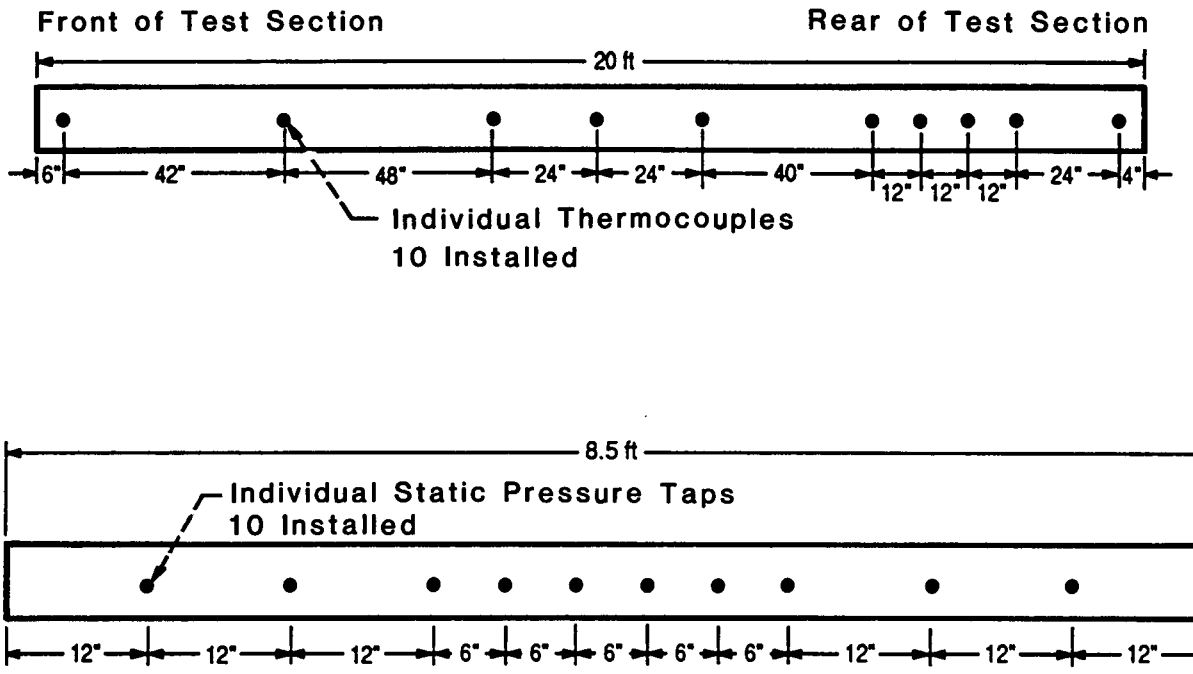

FIGURE 14. - DETAILS OF THE TEST SECTION THERMOCOUPLE AND STATIC PRESSURE INSTRUMENTATION STRIPS.

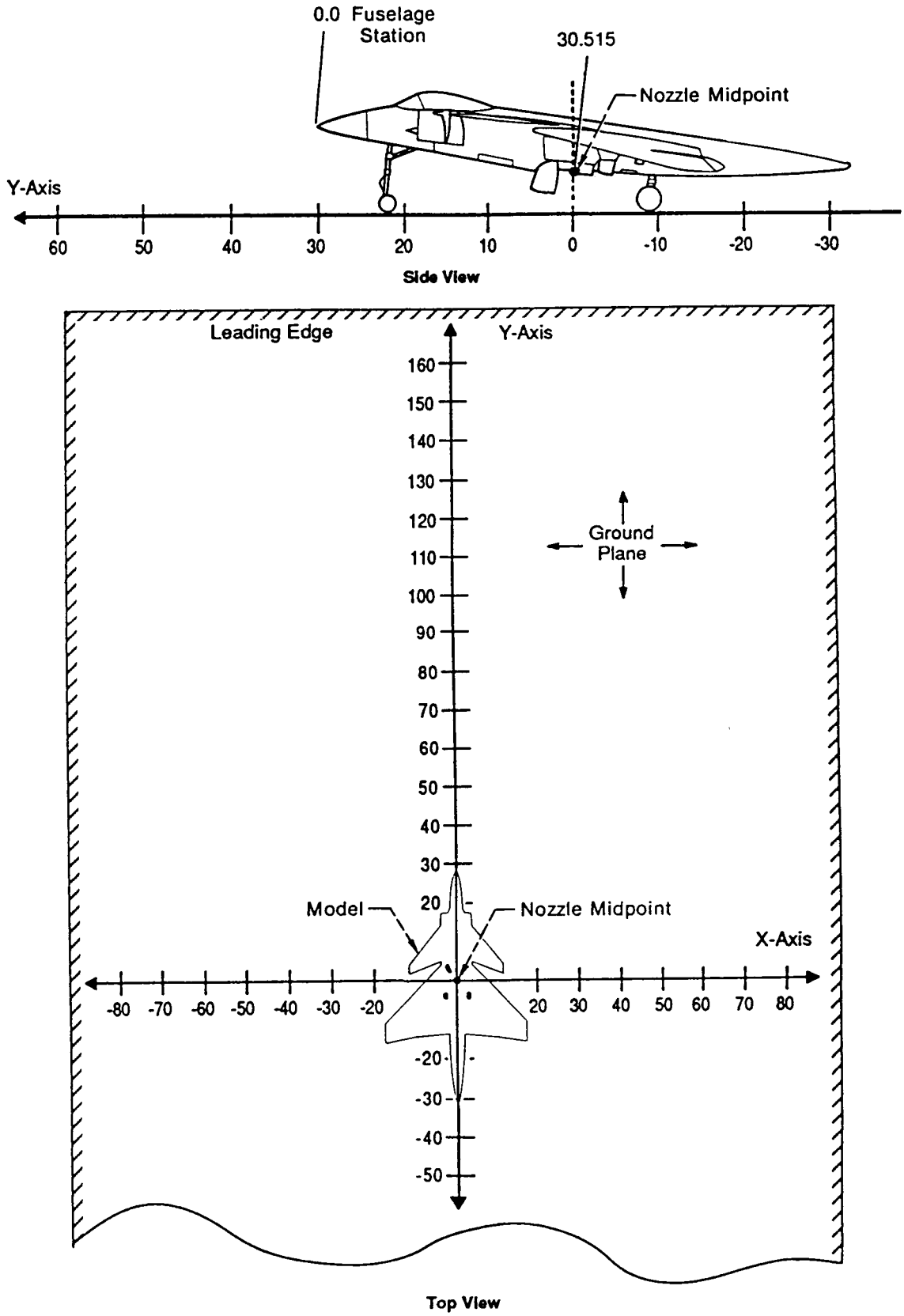

FIGURE 15. - GROUND PLANE COORDINATE SYSTEM AND MODEL LOCATION.

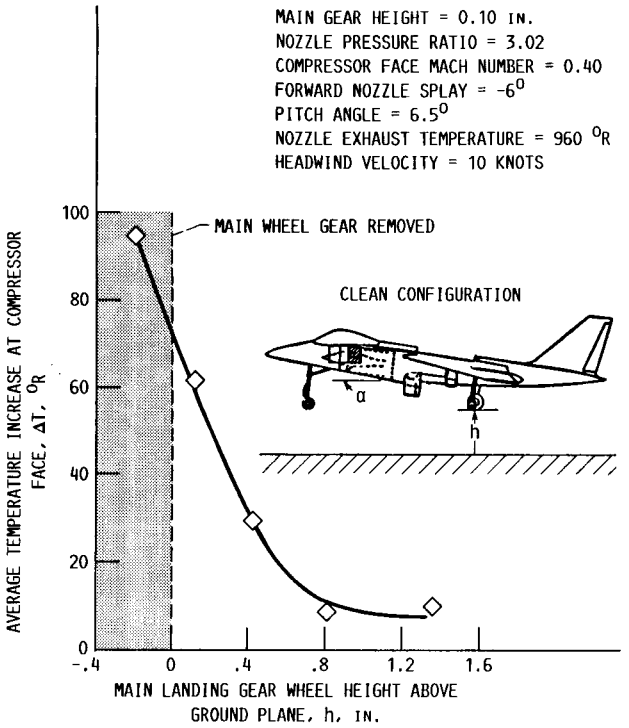

FIGURE 16. - THE MODEL HEIGHT ABOVE THE GROUND PLANE EFFECTS ON HOT GAS INGESTION.

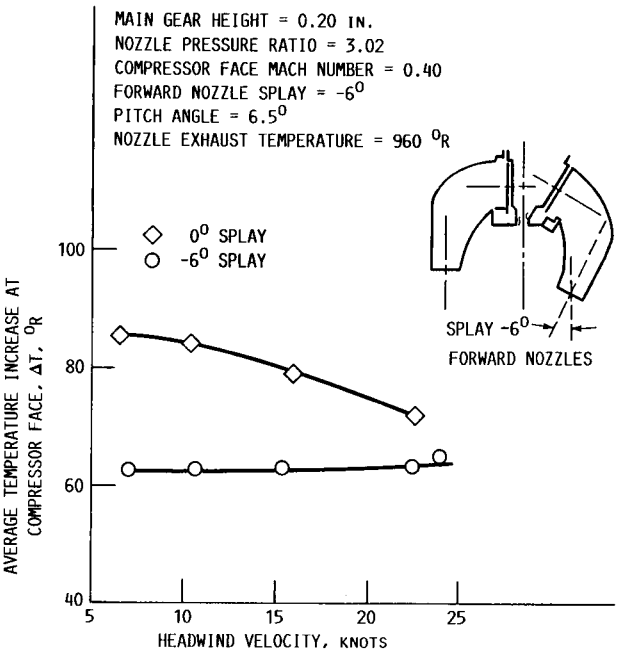

FIGURE 17. - THE EFFECT OF FORWARD NOZZLE SPLAY ANGLE ON HOT GAS INGESTION.

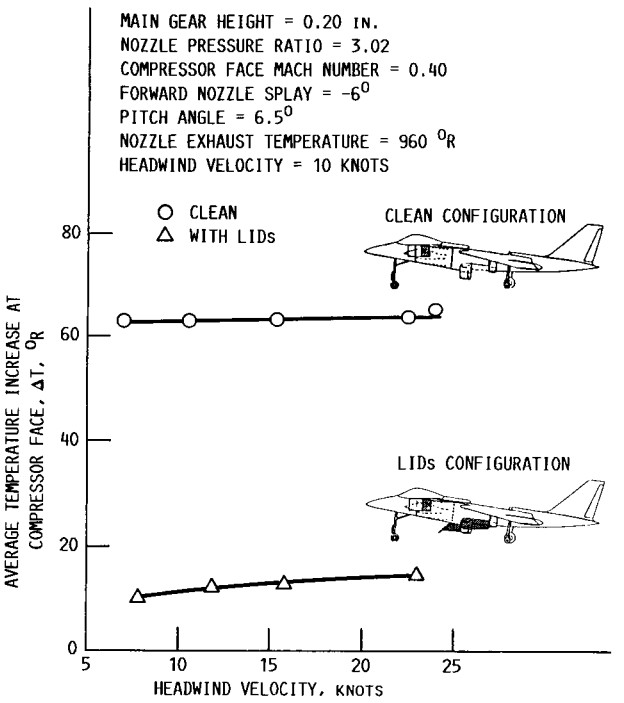

FIGURE 18. - THE EFFECT OF LIFT IMPROVEMENT DEVICES ON HOT GAS INGESTION.

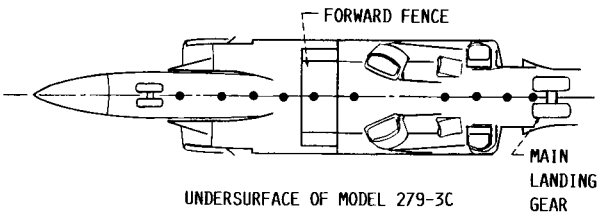

UNDERSURFACE OF MODEL 279-3C

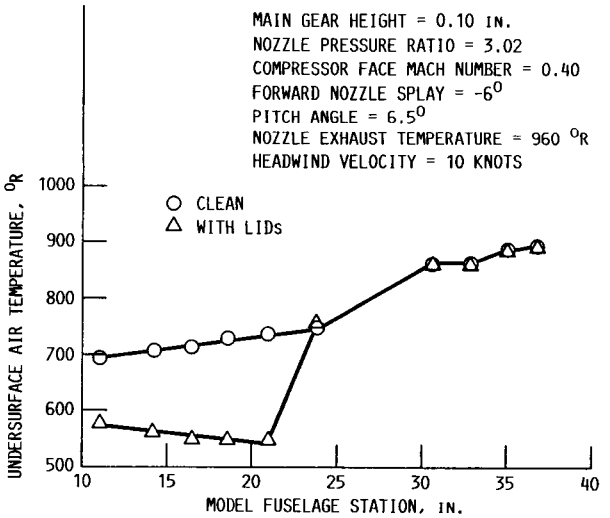

FIGURE 19. - THE EFFECT OF LIDs ON THE MODEL UNDERSURFACE CENTERLINE AIR TEMPERATURE DISTRIBUTION.

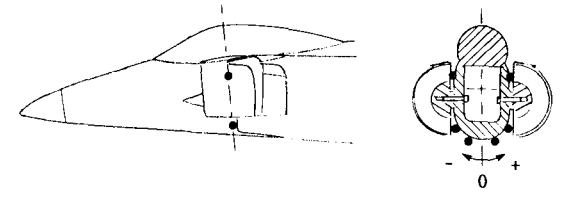

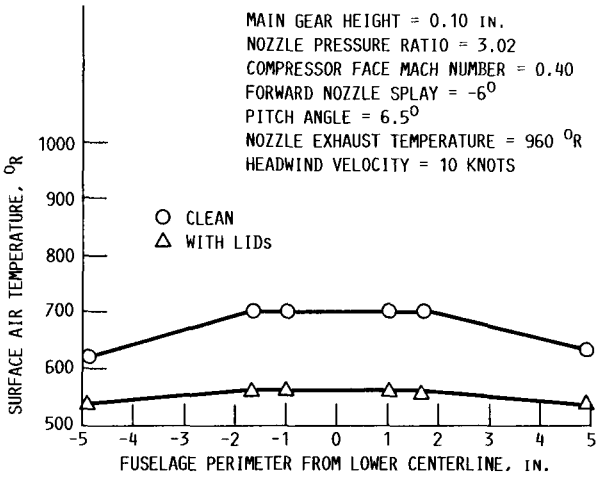

FIGURE 20. - THE EFFECT OF LIDs ON THE TEMPERATURE DISTRIBUTION IN THE INLET PERIMETER REGION.

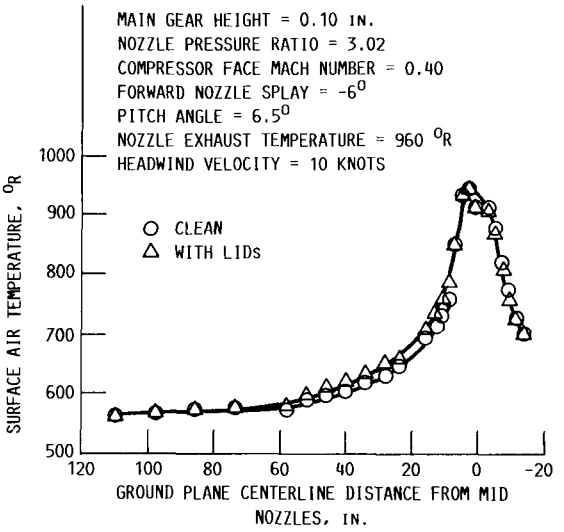

FIGURE 21. - THE GROUND PLANE CENTERLINE AIR TEMPERATURE DISTRIBUTIONS FOR THE CLEAN AND WITH LIDs CONFIGURATIONS.

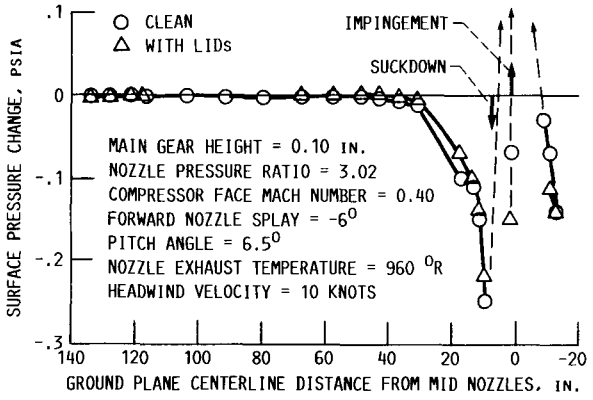

FIGURE 22. - THE GROUND PLANE CENTERLINE PRESSURE CHANGE DISTRIBUTIONS FOR THE CLEAN AND WITH LIDs CONFIGURATIONS.

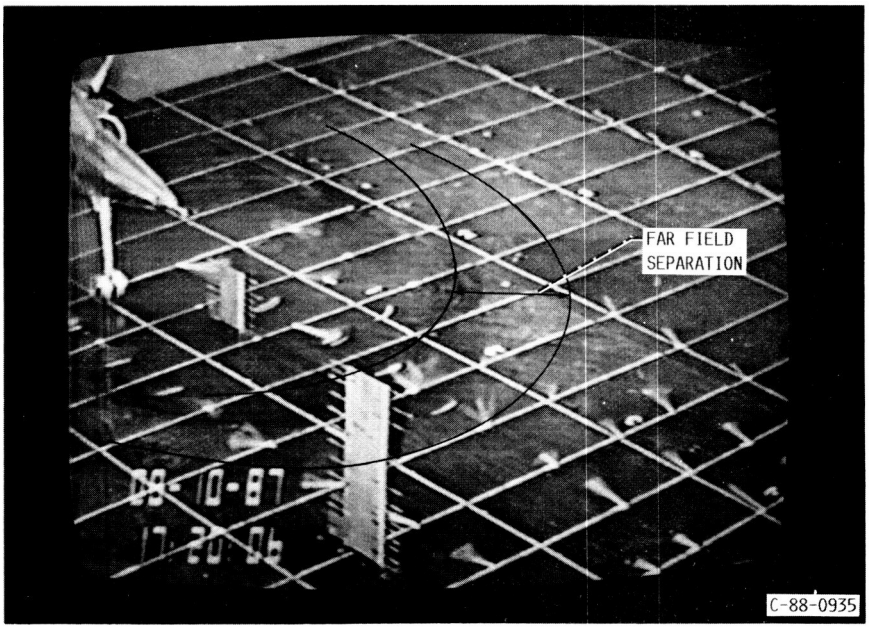

FIGURE 23. - A FLOW VISUALIZATION VIEW SHOWING FAR FIELD SEPARATION AHEAD OF THE MODEL.

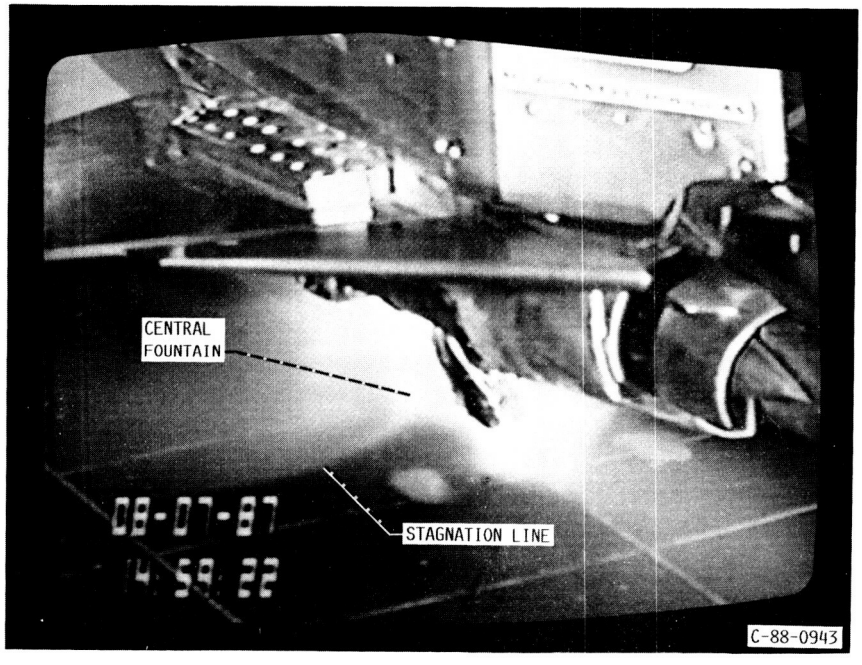

FIGURE 24. - A THREE-QUARTER VIEW OF THE CLEAN CONFIGURATION SHOWING THE NEAR FIELD CENTRAL FOUNTAIN/LOCAL FLOW FIELD CHARACTERISTICS.

NASA
National Aeronautics and Space Administration

Report Documentation Page

1. Report No.	2. Government Accession No.	3. Recipient's Catalog No.
NASA TM-100952 AIAA-88-3025		

4. Title and Subtitle

Hot Gas Ingestion Testing of an Advanced STOVL Concept in the NASA Lewis 9- by 15-Foot Low Speed Wind Tunnel With Flow Visualization

5. Report Date

6. Performing Organization Code

7. Author(s)

Albert L. Johns, Joseph D. Flood, Thomas W. Strock, and Kurt C. Amuedo

8. Performing Organization Report No.

E-4250

10. Work Unit No.

505-62-71

9. Performing Organization Name and Address

National Aeronautics and Space Administration
Lewis Research Center
Cleveland, Ohio 44135-3191

11. Contract or Grant No.

13. Type of Report and Period Covered

Technical Memorandum

12. Sponsoring Agency Name and Address

National Aeronautics and Space Administration
Washington, D.C. 20546-0001

14. Sponsoring Agency Code

15. Supplementary Notes

Prepared for the 24th Joint Propulsion Conference cosponsored by the AIAA, ASME, SAE, and ASEE, Boston, Massachusetts, July 11-13, 1988. Albert L. Johns, NASA Lewis Research Center; Joseph D. Flood, Thomas W. Strock, and Kurt C. Amuedo, McDonnell Aircraft Company, McDonnell Douglas Corporation, St. Louis, Missouri 63166.

16. Abstract

Advanced Short Takeoff/Vertical Landing (STOVL) aircraft capable of operating from remote sites, damaged runways, and small air capable ships are being pursued for deployment around the turn of the century. To achieve this goal, it is important that the technologies critical to this unique class of aircraft be developed. Recognizing this need, NASA Lewis Research Center, McDonnell Douglas Aircraft, and DARPA defined a cooperative program for testing in the NASA Lewis 9- by 15-Foot Low Speed Wind Tunnel (LSWT) to establish a database for hot gas ingestion, one of the technologies critical to STOVL. This paper will present a few results from a test program along with a discussion of the facility modifications allowing this type of testing at model scale. These modifications to the tunnel include a novel ground plane, an elaborate model support which included four degrees of freedom, heated high pressure air for nozzle flow, a suction system exhaust for inlet flow, and tunnel sidewall modifications. Several flow visualization techniques were employed including water mist in the nozzle flows and tufts on the ground plane. Headwind (freestream) velocity was varied from 8 to 23 knots.

17. Key Words (Suggested by Author(s))	18. Distribution Statement
STOVL Vectored thrust Hot gas ingestion Flow visualization	Unclassified – Unlimited Subject Category 02

19. Security Classif. (of this report)	20. Security Classif. (of this page)	21. No of pages	22. Price*
Unclassified	Unclassified	26	A03

*For sale by the National Technical Information Service, Springfield, Virginia 22161